Comparative study of inclusion complex formation between β-cyclodextrin (host) and aromatic diamines (guests) by mixing in hot water, co-precipitation, and solid-state grinding methods

JOURNAL OF CARBOHYDRATE CHEMISTRY
https://doi.org/10.1080/07328303.2022.2068026

Comparative study of inclusion complex formation between β-cyclodextrin (host) and aromatic diamines (guests) by mixing in hot water, co-precipitation, and solid-state grinding methods

Mohammed Jabedul Hoque[a], Mitsuo Toda[b], and Nobuyuki Mase[a,b,c]

[a]Department of Optoelectronics and Nanostructure Science, Graduate School of Science and Technology, Shizuoka University, Hamamatsu, Japan; [b]Department of Engineering, Graduate School of Integrated Science and Technology, Shizuoka University, Hamamatsu, Japan; [c]Research Institute of Green Science and Technology, Shizuoka University, Hamamatsu, Japan

ABSTRACT

Aromatic diamines are essential components of polyimide and many other thermosetting polymers. Recent attention has been growing on the threading of cyclodextrins (CDs) onto diamine monomers intended to improve the solubility in water and thermal stability of resultant polymers. The co-precipitation method is often used to isolate inclusion complexes (ICs) of aromatic diamines and other sparingly water-soluble aromatic guest molecules with β-CD. To find the viability of other methods, we studied IC formation between β-CD and some aromatic diamines by mixing in hot water, co-precipitation, and solid-state grinding. ICs formation in water was carried out by solid guest dispersion into the β-CD aqueous solution at 80 °C with high-speed magnetic stirring. In contrast, solid-state grinding was employed by adding a small amount of water to promote IC formation. Thus, ICs prepared by mixing in hot water and solid-state grinding methods were crystallized from water by cooling to 4 °C. Structures of the ICs in solution were confirmed by chemical shifts changes of cavity protons of β-CD in ^{1}H NMR and the cross-peaks between aromatic protons and cavity protons in ^{1}H-^{1}H ROESY NMR. Job's plot and NMR titration experiments were used to determine the stoichiometric ratio of host and guest in solution.

ARTICLE HISTORY
Received 4 November 2021
Accepted 28 March 2022

KEYWORDS
Aromatic diamines; crystallization; cyclodextrin; inclusion complexes

CONTACT Mohammed Jabedul Hoque pg528989@cii.shizuoka.ac.jp Department of Optoelectronics and Nanostructure Science, Graduate School of Science and Technology, Shizuoka University, 3-5-1 Johoku, Hamamatsu, Shizuoka 432-8561, Japan; Mitsuo Toda toda.mitsuo@shizuoka.ac.jp Department of Engineering, Graduate School of Integrated Science and Technology, Shizuoka University, 3-5-1 Johoku, Hamamatsu, Shizuoka 432-8561, Japan.

Q1 Supplemental data for this article can be accessed on the publisher's website

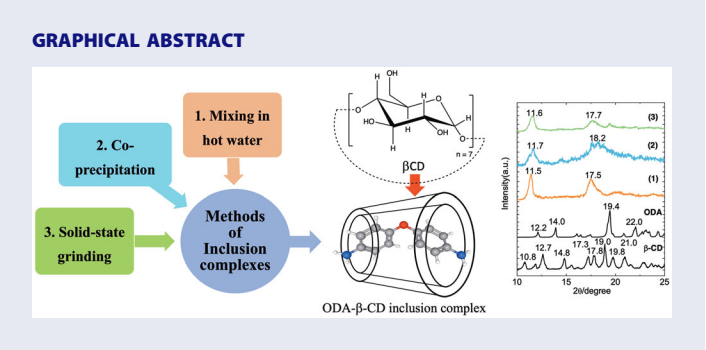

Introduction

Cyclodextrins (CDs) are cage-like macromolecular hosts used in drug formulations, surfactants, and functional materials.[1,2] CDs form inclusion complexes (ICs) with diverse hydrophobic guests through non-covalent interactions, such as hydrogen bonds and hydrophobic interactions.[3,4] Formation of ICs strongly affects the physicochemical properties of guest molecules through shielding effects or restriction of movement.[5] IC formation depends on the geometrical fitting between the CD cavity and guest molecule, as well as the nature of the solvent. In polar organic solvents, IC formation is under equilibrium between threading and dethreading. In contrast, in water, ICs are formed because the hydrophobic environment of the CD cavity is convenient for hydrophobic guests.[6–9]

Aromatic diamines, such as 4,4′-oxydianiline (ODA), 4,4′-methylenedianiline (MDA), 1,4-phenylenediamine (PD), and 2,2-bis[4-(4-aminophenoxy)phenyl]propane (BAPP), are widely used as monomers for synthesizing polyimide, polyamide, polyurethane, and polyhemiaminal thermosetting polymers.[10–13] In contrast, spacer containing aromatic diamines, such as 1,2-bis(4-aminophenoxy)ethane (BAPE) and 1,4-bis(4-aminophenoxy)butane (BAPB), are used to improve the flexibility of polymers.[14] Unless functionally modified, thermosetting polymers often suffer from poor solubility owing to their high cross-link densities. The incorporation of CDs into thermosetting polymers, such as polyimide, polyamide, fullerene, and polyaniline, has been reported to enhance the solubility and thermal stability of thermosetting polymers.[7–10] In general, the synthesis of CDs containing polymers is performed by the inclusion of CDs into aromatic diamines followed by a polycondensation reaction. Various methods have been established for the preparation of ICs as solids, such as co-precipitation, freeze-drying, kneading, and solid-state grinding.[15,16] Co-precipitation method is typically used to prepare CD-ICs of various aromatic diamines and other aromatic guests.[17,18] In the co-precipitation method,

COLOR Online / B&W in Print

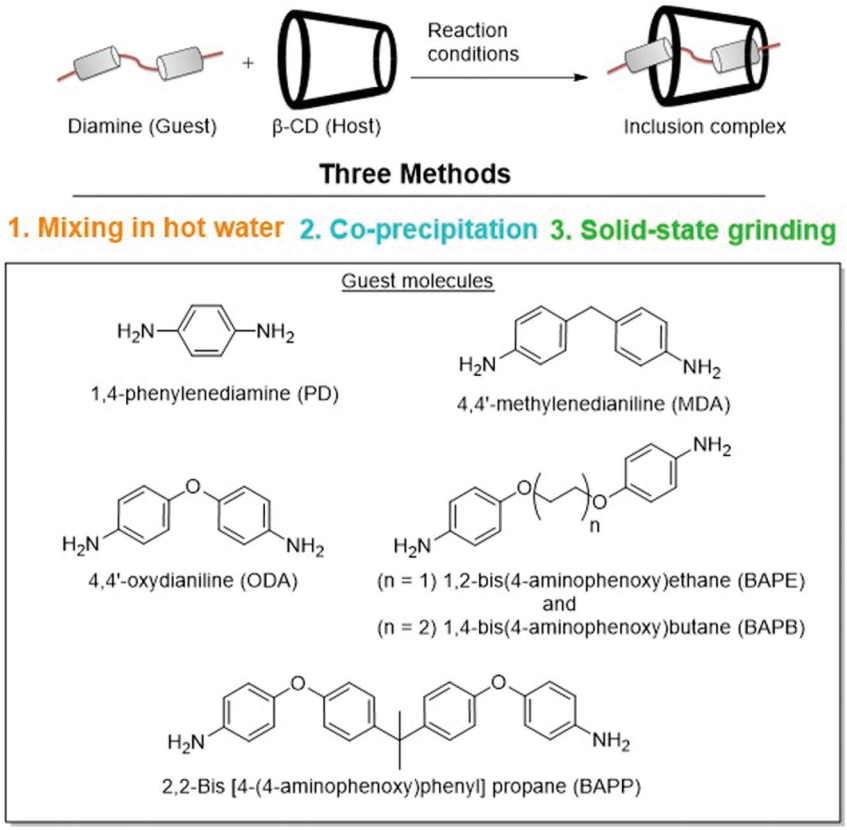

Scheme 1. The synthetic scheme of ICs formed between aromatic diamines (guests) and β-CD (host) by mixing in hot water, co-precipitation, and solid-state grinding methods.

IC formation of CDs with aromatic guests is achieved by the co-precipitation of complexes in a mixture of water and alcohol. In this process, alcohol is used to diffuse the guest molecules into an aqueous CD solution, and the reaction is accomplished through IC precipitation. As CDs have a large hydroxyl surface, complete dissolution of guests in co-solvent is unnecessary, and the simple dissolution of CDs and aromatic guests in hot water could afford ICs. To solve this issue, we investigated the preparation method of ICs, such as crystallization in water, as well as solid-state grinding (Scheme 1).

IC formation in hot water is a reliable method because the co-solvent is eliminated. In this case, IC formation is favored by entropy-driven water molecule ejection from the CD cavity and hydrophobic interaction at high temperatures.[19] Notably, aliphatic polyether amines and polyethylene glycol-based ICs with many threaded CDs form a precipitate in water due to CD aggregation in a single chain and hydrogen bonding among neighboring CDs.[4] However, small molecules, such as ODA and MDA, which have

few threaded CDs, could offer soluble ICs in water due to free CD hydroxyl groups. On the other hand, solid-state grinding is also an efficient method of IC formation between small drug molecules and CD.[15,16] In this process, strong mechanical force is applied in the form of friction to the host-guest mixture to obtain IC with respect to grinding time.

Further, a comparative study has been made based on results obtained from three different methods, mixing in hot water, co-precipitation, and solid-state grinding, to rationalize the most suitable method for IC formation of aromatic diamines and β-CD. IC formation and structure of the complexes were confirmed by NMR, FTIR, and XRD. Job's plot (a continuous variation method) and NMR titration methods were applied to determine the host-guest stoichiometric ratio of ICs in solution.[20] Elemental analysis was used to determine the composition of ICs. The thermal characteristics were evaluated by differential scanning calorimetry (DSC) and thermogravimetric analysis (TGA).

Results and discussion

To find the suitable method of IC formation of aromatic diamines and β-CD, three different methods, including mixing in hot water, co-precipitation, and solid-state grinding were studied. In this research, six different aromatic diamines, including PD, MDA, ODA, BAPE, BAPB, and BAPP, were used as guests of the β-CD host (Scheme 1). Among those diamines, PD and MDA are reported to be soluble in water (PD = 40 mg/mL and MDA = 1 mg/mL at 25 °C) according to the PubChem database system. No water solubility report was available for other studied diamines. It is important to know the initial solubility of guest molecules before studying their IC formation with β-CD.

According to the co-precipitation method, IC formation was carried out by diffusing an aromatic diamine solution in ethanol or methanol into the aqueous solution of β-CD at room temperature for 24 h followed by precipitating on cooling at 4 °C.[18] Thereafter, the precipitates obtained were collected and characterized.

To assess the advantages of the large hydroxyl surface of CDs, IC formation was carried out in hot water by adding solid guest directly into β-CD aqueous solution. Herein, we describe a simple four-step procedure including high dilution synthesis of ICs at 80 °C for 24 h, filtration, evaporation of excess water at 50 °C, and crystallization on cooling at 4 °C to afford IC crystals (Schemes 1 and 2). High dilution conditions with portion-wise addition of solid guests under high-speed magnetic stirring at high temperature render the solubility of hydrophobic aromatic diamines. Conceptually, during the inclusion process, a microenvironment exists in

COLOR Online / B&W in Print

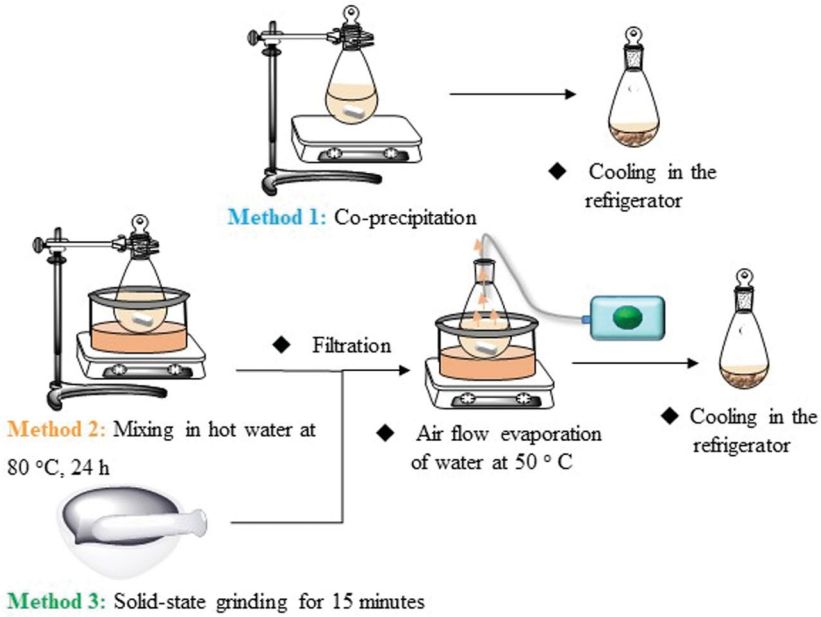

Scheme 2. Schematic representation of ICs formation between aromatic diamines (guests) and β-CD (host) by mixing in hot water, co-precipitation, and solid-state grinding methods. Details procedure is included in the supporting information.

water with a balance between hydrophobic and hydrophilic partners. As soon as hydrophobic guests enter the hydrophobic host cavity of CD, a dominant hydrophilic environment leads to the dissolution of hydrophobic guests in water. After workup to remove excess water, the high IC concentration in the solution could trigger crystallization, as decreasing solvent volume generally results in a concentration gradient that promotes crystallization.[21,22] Furthermore, to determine the effect of the β-CD amount on IC formation, the molar feed ratios of β-CD relative to ODA and MDA (1:1, 2:1, 3:1), PD (1:1, 1/2:1, 1/4:1), BAPE, and BAPB (1:1, 2:1, 3:1), and BAPP (2:1) were varied. Thus, ICs and the mixture of IC and excess components obtained by all the studied diamines were represented in supporting information (Fig. S1A). Notably, above the molar feed ratio of 2:1 for ODA-β-CD and MDA-β-CD, some large aggregates of β-CD were observed due to a mixture of ICs and excess β-CD (Fig. S1B). These large aggregates were identical to β-CD crystals obtained from the recrystallization in water by dissolving in hot water and then cooling at 24 °C for a week (Fig. S1C). Notably, the percent weight of large crystals separated from the mixture of MDA-β-CD and β-CD (molar feed ratio 2:1 and 3:1) were ∼36.2 and 68.7% of the total weight of solid crystals (Fig. S1B).

Apart from the methods of co-precipitation and mixing in hot water for IC formation, the solid-state grinding method was also applied. To do so, a

host-guest mixture (0.4 g scale) was ground with 0.25 mL of water (to make a slurry) for 15 min, and then the mixture was suspended in 10 mL of water and heated for 30 min at 50 °C and filtered. The resultant complex solution was extracted and then crystallized by cooling at 4 °C. IC crystals obtained from the filtrate portions were considered for percent yield calculation.

Crystals obtained from the above three methods were denoted as follows: PD–β-CD, ODA–β-CD, MDA–β-CD, BAPE–β-CD, BAPB–β-CD, and BAPP–β-CD. Among them, BAPP–β-CD was precipitated during the reaction workup due to the low solubility of BAPP. This is possible because of the hydrophobic domination of $-C(CH_3)_2-$ groups in BAPP. However, crystals isolated from the filtrate portion of the BAPP–β-CD complex mixture were found to be β-CD. Percent yield was calculated based on β-CD (Table S1). Molar feed ratios of host and guest were correlated with NMR integral ratios of ICs. Both ODA–β-CD and MDA–β-CD obtained by three methods showed an integral ratio of ~0.9 (theoretically, 7H/8H = 0.875), at a molar feed ratio of 1:1 (β-CD:diamine), which indicated the formation of ICs. In contrast, PD–β-CD crystals isolated from water showed an integral ratio of 2.0 (host:guest = 1:1, theoretically, 7H/4H = 1.75), at a molar feed ratio of 1:4, which is presumably due to the high solubility of PD (40 mg/mL in water) in the free state. However, host-guest ratios of BAPE–β-CD were varied with the increase of β-CD molar amount. Also, different host-guest ratios were observed between hot water and co-precipitation methods. This is probably due to the mixture ICs and excess β-CD. However, β-CD integral ratio calculated from various molar feed ratio products of BAPE–β-CD and BAPB–β-CD were randomly changing, which indicated that an excess amount of β-CD was crystallized with ICs. Notably, a mixture of ICs and excess β-CD was obtained by solid-state grinding between β-CD and BAPE or BAPB diamines at different grinding times (15, 30, 45, and 60 min), confirmed by the ROESY NMR analysis. In this case, the addition of a small amount of water and different grinding times were evaluated to overcome the issues of the slow diffusion problem of large guest molecules (BAPE, BAPB, and BAPP).[23] In contrast, PD, ODA, and MDA had readily formed ICs by the solid-state grinding method.

^{1}H NMR and ^{13}C NMR assay of ICs

^{1}H NMR is an essential tool to study the structure of CD ICs.[24] IC formation was evidenced by chemical shift changes of both aromatic protons and the cavity protons due to the ring current effect of the aromatic system.[25] Observed chemical shift changes and broadening of CD peaks can give insight into the information of conformational changes of supramolecular assemblies. Typically, six different proton peaks were assigned for β-CD in

D_2O, such as H_1 doublet at 4.92 ppm, H_3 doublet of doublet at 3.81 ppm, H_6 multiplet at 3.72 ppm, H_5 multiplet at 3.70 ppm, H_2 doublet of doublet at 3.50 ppm, and H_4 doublet of doublet at 3.43 ppm, respectively (Fig. S2). Despite the low water solubility of studied diamines, NMR measurement (in D_2O) was carried out to assign their proton peaks and to compare them with ICs. To do so, each diamine was suspended in D_2O and the vial was heated at 80 °C for 24 h while stirring magnetically. ODA, BAPE, and BAPB solutions were syringe filtered and subjected to NMR measurement. Among the diamines, MDA, ODA, and PD spectra were recorded successfully (Figs. S2a–c). However, BAPE, BAPB, and BAPP diamines exhibited very low-intensity peaks due to the low solubility in D_2O. Furthermore, ^{1}H NMR of ODA-β-CD, MDA-β-CD, BAPE-β-CD, BAPB-β-CD, PD-β-CD crystals was recorded in D_2O (Figs. S2d–h). However, BAPP-β-CD was recorded in DMSO-d_6 due to low solubility in D_2O (Figs. S2d–n). Complex induced chemical shift changes were listed in Table 1. Host-guest ratios of ICs were calculated from integral ratios (Table S1). Further, ^{1}H NMR titration method was used to study the ICs formed between β-CD and some diamines (MDA, PD, and BAPE) (Figs. S2j–m). Significant shifts in the ^{1}H NMR resonances of the cavity protons (H_3 and H_5) of β-CD were observed in MDA–β-CD ICs prepared by all three methods, indicating a conformational change of β-CD upon ICs formation (Figs. 1A–F). Notably, the biggest up-field shifts for H_3 and H_5 protons were observed with H_5 cavity protons located along the narrow rim, indicating shallow penetration of the guest molecules inside the cavity. Also, the methylene protons of MDA have suffered a significant up-field shift with suppression of intensity by the cavity protons of β-CD. However, no significant difference in chemical shifts was observed among the three preparation methods as well as direct mixing of equimolar amounts of MDA and β-CD in D_2O, indicating the identical complex structure (Figs. 1C–F). In contrast, a mixture of IC and

Table 1. Complexation-induced chemical shift changes (CICS $= \delta_{host} - \delta_{complex}$) of the ICs. H_3 and H_5 are cavity protons whereas H_1 and H_6 are outer protons.

	Changes of chemical shifts of β-CD			
Compounds and method[a]	H_1	H_3	H_5	H_6
ODA-β-CD (HW)	0.0079	0.1175	0.2594	0.0750
ODA-β-CD (CP)	−0.0076	0.1044	0.2432	0.0617
ODA-β-CD (SG)	0.0131	0.1213	0.2757	0.0799
MDA-β-CD (HW)	−0.0261	0.0566	0.2357	0.0678
MDA-β-CD (CP)	−0.0290	0.0495	0.2315	0.0645
MDA-β-CD (SG)	−0.0388	0.0367	0.2296	0.0495
PD-β-CD (HW)	−0.0041	0.0077	−0.0024	0.0268
PD-β-CD (CP)	0.0036	0.0284	0.0429	0.0124
PD-β-CD (SG)	−0.0046	0.0068	−0.0029	0.0254

The negative sign indicates the downfield shift (deshielding).
[a]Abbreviations for the three preparation methods: mixing in hot water (HW), co-precipitation (CP), and solid-state grinding (SG).

COLOR Online / B&W in Print

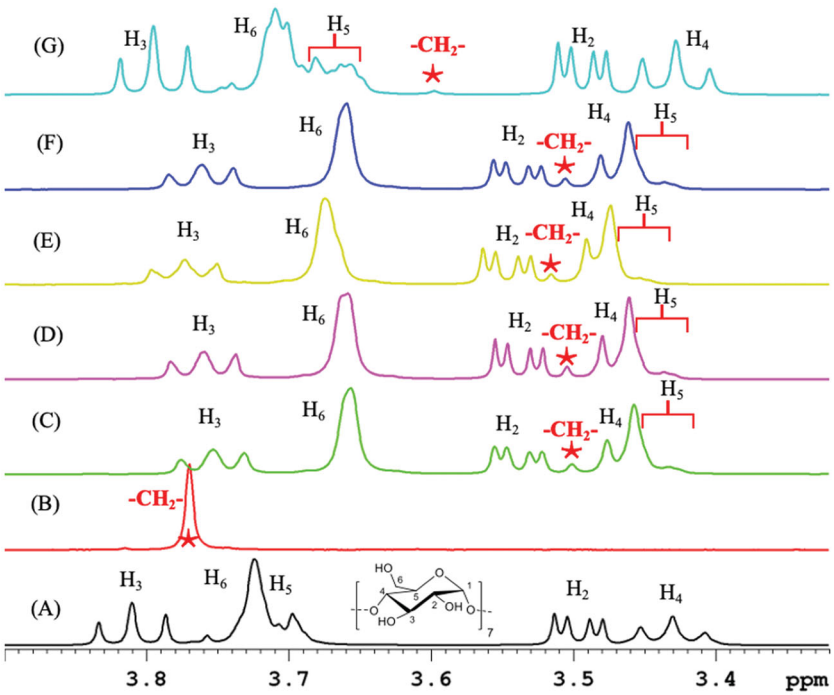

Figure 1. ^{1}H NMR spectra (400 MHz, in D_2O, 298 K, internal standard DSS-d_6) of (A) β-CD (B) MDA and MDA-β-CD prepared by three methods, such as (C) mixing in hot water (D) co-precipitation (E) solid-state grinding for 15 min (F) mixing equimolar amount of MDA and β-CD in D_2O (G) MDA-β-CD complex mixture obtained from molar feed ratio 3:1 (Host: Guest).

excess components obtained from molar feed ratio 3:1 (Host:guest) was lack of complete chemical shift changes due to an excess amount of β-CD (Fig. 1G). Similarly, ^{1}H NMR titration of MDA by β-CD indicated an initial increase of chemical shift of H_5 protons at molar ratios of MDA/β-CD at 0.94 followed by a decrease at 0.47, 0.31, 0.24, and 0.19 (Fig. S2j).

A similar trend of chemical shift changes was observed in the ^{1}H NMR titration spectra of PD and β-CD (Fig. S2k). However, BAPE and β-CD titration spectra recorded at 25 and 80 °C showed a well resolved up-field shift of methylene proton peaks (Figs. S2l,m). Further, ^{1}H NMR titration graphs plotted based on chemical shift changes of β-CD protons indicated the formation of 1:1 complex between β-CD and some diamines, such as MDA, PD, and BAPE (Figs. S2n–p). However, the largest up-field shifts among the studied diamines were observed for H_5 protons of ODA-β-CD ICs, indicating the change of symmetry of ODA inside the β-CD cavity (Table 1, Fig. S2e). The integral ratio of MDA–β-CD prepared by the molar feed ratio of MDA:β-CD (1:1 and 1:2.0) was found to be 0.88 and 1.01, indicating that the 1:1 complex was formed (Table S1). Similar integral ratios (0.90 and 0.96) were observed for ODA-β-CD ICs prepared at a molar feed ratio of ODA: β-CD (1:1 and 1:1.5). On the other hand, small

chemical shift changes were observed in BAPE–β-CD and BAPB–β-CD due to the mixture of ICs and excess β-CD.[26,27] Integral ratio calculation reveals the host-guest ratio of BAPE–β-CD prepared by mixing in water and co-precipitation methods are 3:1 and 5:1, which was associated with high β-CD content in the complex mixture. Such high ratio complexes are also associated with low solubility of BAPE and high solubility of β-CD. Despite the host-guest ratios of 3:1 and 5:1, only equivalent proton peaks were observed for the monosaccharide pattern of β-CD, which was probably due to the fast equilibrium between association and dissociation relative to the NMR time scale.[28] Also, it was reported that CD motion around the guest causes the average monosaccharide pattern of CD in the NMR spectrum.[29] Further, low-temperature (up to 5 °C) NMR measurement was not successful to separate a mixture of proton peaks except for peak broadening due to the viscosity effect. However, a combined ^{1}H NMR (in D_2O) spectra of BAPE, a mixture of BAPE and β-CD, and BAPE–β-CD solid product obtained by mixing in water were used to evaluate the mixture of products (Fig. S2g). Typically, BAPE showed extremely low-intensity aromatic peaks due to low solubility in water. In contrast, an equivalent mixture of BAPE and β-CD in D_2O at 25 °C showed a host and guest ratio of 4.1 due to soluble fraction containing IC and excess β-CD. Similarly, a host and guest ratio of 3.6 was observed in BAPE–β-CD prepared by mixing in hot water at 80 °C. However, a high temperature is required to increase the complexation rate and yield.

On the other hand, PD-β-CD prepared at molar ratios 1:1 and 1/2:1 showed less intense aromatic peaks in the ^{1}H NMR spectrum owing to the full coverage of PD by the β-CD.[10] Hence, the host-guest ratio calculation remains ambiguous. In contrast, aromatic proton peaks of PD-β-CD solid prepared at a molar feed ratio of 1:4 (β-CD: PD) were well resolved and the integral ratio was found ∼2.0 (theoretically 1.87), indicating a host-guest ratio of 1:1 in PD-β-CD ICs (Fig. S2h). However, the host-guest ratio of BAPP-β-CD (in DMSO-d_6) prepared by mixing in hot water was found to be 1:1, which is presumably due to the 3 D bend structure of BAPP (Fig. S2i). Such structural strain could inhibit the multiple β-CD threading as well as low water solubility of the ICs. However, a host-guest ratio of 1:2 was found for BAPP-β-CD prepared by the co-precipitation method due to a mixture of IC and excess β-CD aggregation. Notably, there is a possibility of β-CD threading onto -$C(CH_3)_2$- groups.

In the meantime, complexation-induced ^{13}C NMR chemical shift changes were also observed in the ICs (Fig. S3). In the ^{13}C NMR of ODA–β-CD and MDA–β-CD ICs, significant downfield chemical shifts of the cavity carbons (C3 and C5) were observed due to the threading of β-CD onto ODA and MDA (Figs. S3a–d). However, a significant up-field shift was observed for PD–β-CD ICs, which is indicating that the relative position of PD at the

narrow rim (Fig. S3). Also, it was reported that guest molecules, such as benzoic acid having in-depth penetration in the CD cavity undergo shielding of ^{13}C NMR peaks.[24] However, chemical shift changes of the cavity carbons were barely observed for the mixture of products obtained from BAPE, and BAPB with high β-CD content.

^{1}H-^{1}H ROESY NMR analysis of ICs

Furthermore, ^{1}H-^{1}H ROESY NMR spectroscopy was used to estimate the relative position of guest molecules inside the β-CD cavity of ICs. This experiment reveals the interactions between the CD cavity and the guest molecules. In the ROESY spectrum of MDA–β-CD ICs (1:1 prepared by mixing in hot water) in D_2O, a strong correlation was observed between the aromatic protons at 6.83 (H_Q) and 6.66 (H_P) ppm and the β-CD cavity protons at 3.75 (H_3) and 3.47 (H_5) ppm, confirming the threading of MDA inside the β-CD cavity (Fig. 2A). Apart from the cavity protons, a strong correlation was observed between aromatic protons and H_6 protons linked to the narrow rim of the β-CD, indicating the in-depth penetration of guest molecules inside the β-CD cavity. Similarly, in ^{1}H-^{1}H ROESY spectrums of ODA–β-CD ICs, strong cross-peaks were observed (Fig. S4). Conversely, a small correlation was observed between aromatic protons at 6.81 (H_Q) and 6.46 (H_P) ppm and the β-CD cavity proton at 3.55 (H_5) ppm in ^{1}H-^{1}H ROESY spectrum (DMSO-d_6) of MDA–β-CD ICs, indicating the dissociation of MDA from the cavity (Fig. 2B). Additionally, a simple mixture of β-CD and some diamines (MDA, PD, BAPE, and BAPB) in D_2O exhibited correlation peaks in ^{1}H-^{1}H ROESY analysis. However, correlation peaks were not observed for a simple mixture of β-CD and ODA or BAPP at 25 °C due to the low solubility and slow diffusion of those diamines in D_2O. On the other hand, strong interaction was observed between cavity protons and aromatic protons of BAPE–β-CD and BAPB–β-CD complexes prepared by the three methods, indicating the formation of ICs in the solid products (Fig. 2D and Fig. S4a). Both diamines were found to be deeply penetrated in the β-CD cavity, confirmed by the correlation peaks between aromatic protons and both H_5 and H_6. Notably, instead of two separate pairs of proton peaks, a coalesced peak was observed in BAPE–β-CD, that covered the entire aromatic protons, likely due to different IC conformations in D_2O (Fig. 2D).[27]

Further, BAPE–β-CD complexes prepared by solid-state grinding at 15, 30, 45, and 60 min were subjected to ROESY analysis. In the ROESY spectra, identical correlation peaks were observed (Fig. S4b). Additionally, ROESY analysis of BAPE–β-CD complex prepared by 15 min grinding was carried out by varying dissolution time to investigate the effect of dissolution time on correlation peak pattern of ICs. No significant change was

COLOR Online / B&W in Print

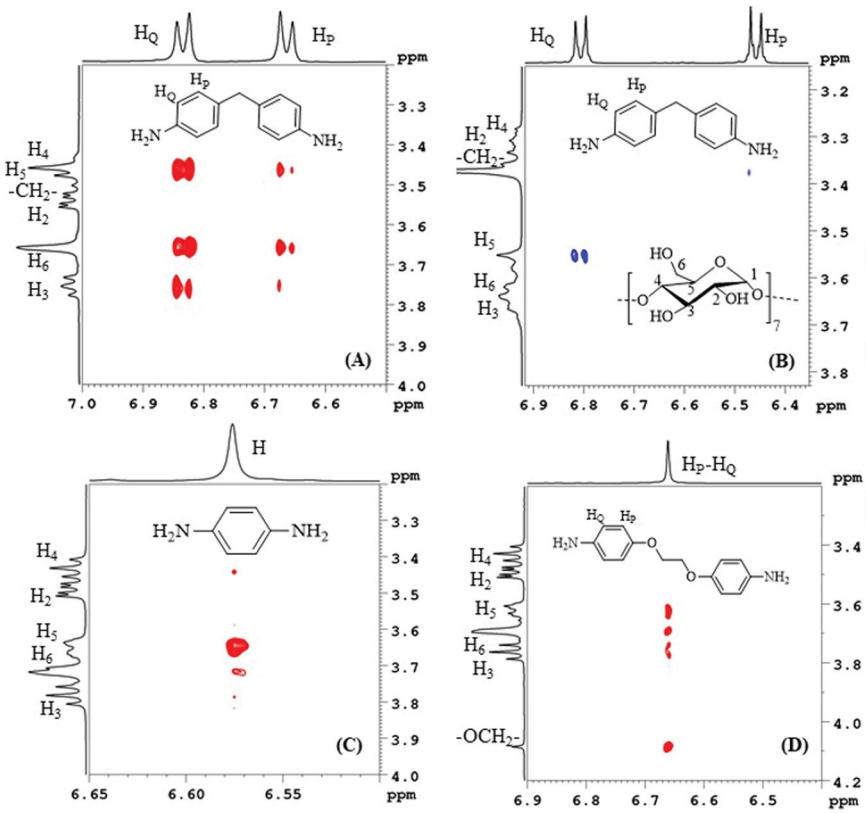

Figure 2. ^{1}H-^{1}H ROESY NMR spectra of MDA-β-CD complex recorded (A) in D_2O (B) in DMSO-d_6, (C) PD-β-CD in D_2O), and (D) BAPE-β-CD in D_2O). ROESY spectrum was recorded by dissolving each complex in D_2O for 10 min (analysis time 50 min).

observed with the increase of dissolution time, indicating the existence of ICs in the solid grinding mixture (Fig. S4c). Similarly, ROESY spectra of BAPB–β-CD complexes prepared by 15 and 30 min grinding times showed significant correlation peaks between cavity protons and aromatic protons (Fig. S4d). On the other hand, intense cross-peaks were observed between aromatic protons of PD and H_5 cavity protons of β-CD, indicating the relative position of PD at the narrow rim of the β-CD cavity (Fig. 4C). In the ROESY spectrum of BAPP–β-CD in DMSO-d_6, no correlation peak was observed owing to the dissociation of β-CD in a polar solvent (Fig. S4e).

FTIR analysis of ICs

FTIR was used to study the ICs obtained by three different methods. In the ICs, the guests were stabilized in the CD cavity, leading to different vibrational modes in the IR region.[18] A representative FTIR spectrum of MDA–β-CD ICs (Fig. 3) was used to evaluate ICs. In the FTIR spectra, the

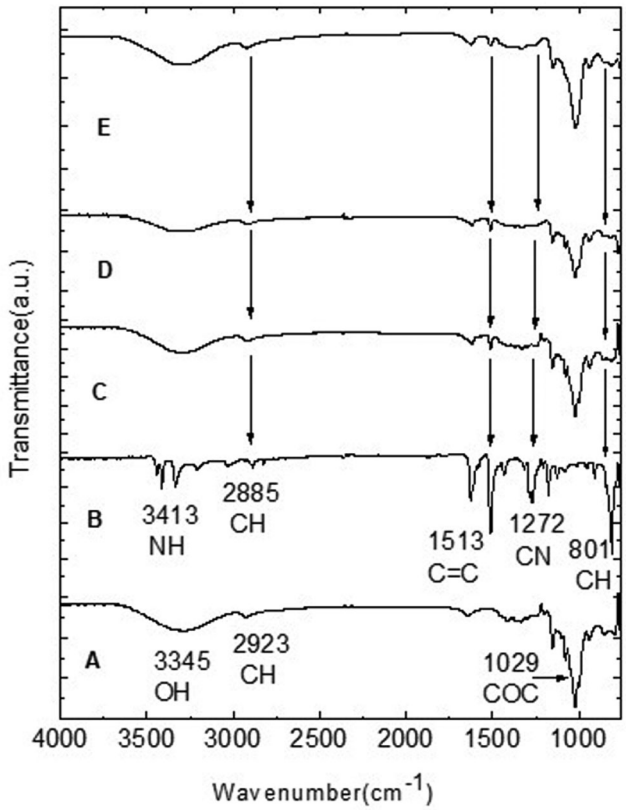

Figure 3. FTIR spectra of (A) β-CD, (B) MDA, and MDA-β-CD prepared by (C) mixing in hot water, (D) co-precipitation, and (E) solid-state grinding for 15 min.

OH stretching band was predominated over the NH stretching band at ~3413 cm^{-1}. Similarly, the intensities of the aromatic stretching band at ~1513 cm^{-1}, CN stretching band at ~1272 cm^{-1}, and aromatic CH bending at ~801 cm^{-1} were decreased due to the low concentration of aromatic diamines in the MDA–β-CD ICs. Moreover, various non-bonding interactions, such as hydrophobic, hydrogen bond, and electrostatic interactions between host and guest lead to the minimization of the energy of the localized part of the guest, thus decreasing the intensities of corresponding bands.[18] In contrast, the aromatic stretching band at ~1499 cm^{-1} and CN stretching band at ~1196 cm^{-1} for ODA–β-CD ICs (1:1) prepared by three methods were well resolved (Fig. S5). On the other hand, an extra band at 1071 cm^{-1} of BAPE and 1046 cm^{-1} of BAPB due to characteristic ether (COC) bond stretching was overlapped by the COC stretching of β-CD (Figs. S5a,b). However, FTIR patterns of both PD–β-CD and BAPP–β-CD were found similar to other diamine complexes (Figs. S5c,d). To distinguish between the physical mixture and solid ICs, a physical mixture was

prepared by grinding β-CD and diamines for 1 min without crystallization. A distinguishable feature was observed between ODA–β-CD and MDA–β-CD ICs prepared in hot water and a physical mixture of ODA and β-CD (Fig. S5e). In this figure, NH stretching and OH stretching appeared as an overlapping band. Also, in this spectrum, aromatic CH bending at ~801 cm^{-1} was not suppressed by the β-CD, which indicated the physical aggregation of β-CD and diamines.[18] To confirm the distribution of β-CDs and aromatic diamines in the isolated products, different portions of the two different ICs of ODA–β-CD (1:1) and MDA–β-CD (1:1) were subjected to FTIR assay (Figs. S5f,g). No significant difference was observed in the fingerprint region.

XRD analysis of ICs

The XRD diffraction pattern of β-CD comprises numerous crystalline peaks in 2θ range of 10–30°, including two characteristic peaks at 10.8 and 12.7° due to cage-type structure.[8,30] Also aromatic diamines showed characteristic crystalline peaks in the 2θ range of 10–30°. Notably, instead of numerous crystalline peaks, two types of broad peaks were observed for MDA–β-CD (1:1) ICs at $2\theta = 11.7°$, 17.7° (in hot water), 11.3°, 17.6° (co-precipitation) and 11.4°, 17.6° (solid-state grinding), indicating that identical crystal structures (channel-type structures) of ICs were produced by three methods (Fig. 4). Identical XRD diffraction patterns of MDA–β-CD ICs prepared by three methods were presumably due to 1:1 ICs being subjected to XRD analysis as well as similar crystallization procedures and drying conditions used to obtain ICs crystals. Similarly, ODA–β-CD ICs showed two types of diffraction peaks at $2\theta = 11.5$, 17.5; 11.7, 18.2, and 11.6°, 17.7°, indicating the characteristic channel-type structure (Fig. S6). In contrast, BAPE–β-CD and BAPB–β-CD exhibited two characteristic peaks at 10.8 and 12.7° associated with a cage-type structure (Figs. S6a,b). This is possibly derived from the mixture of ICs and β-CD. However, It was reported that the crystal structure of β-CD and 4-[2-(4-aminophenyl)ethyl]-benzenamine complex comprises dimeric stacking.[27] Also, an earlier report of α-CD-methyl orange (2:1) complex comprises four possible superposition structures.[26] On the other hand, PD–β-CD prepared by mixing in hot water and in solid-state grinding were found to form channel-type structures, confirmed by characteristic peaks at 11.9, 12.0, 17.7, and 18.8° (Fig. S6c). In contrast, the cage-type structure was observed for PD–β-CD prepared by the co-precipitation method, which is possibly due to the cage-type arrangement of β-CD. Typical, channel-type peaks at around 11.1 and 17.7° were observed for BAPP–β-CD prepared by hot water method and solid-state grinding method (Fig. S6d). However, a different XRD pattern was observed for

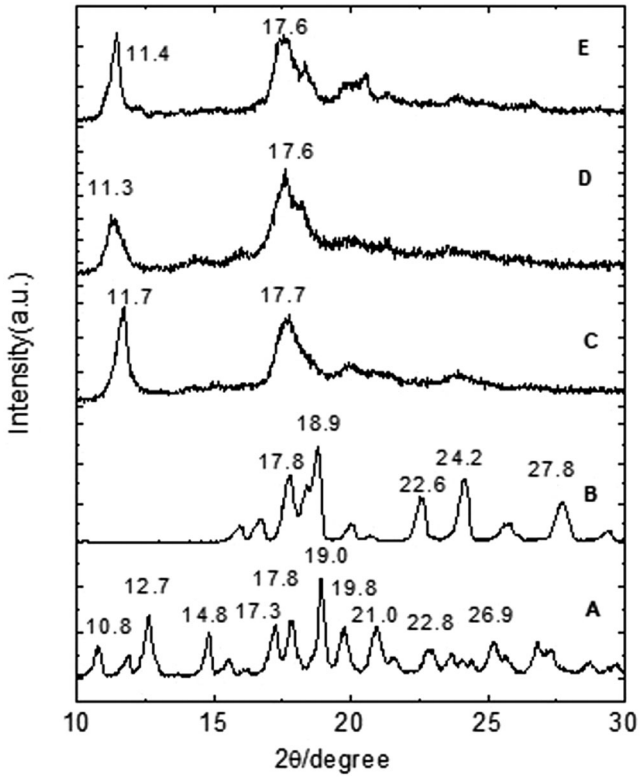

Figure 4. XRD patterns of (A) β-CD, (B) MDA, and MDA-β-CD prepared by (C) mixing in hot water, (D) co-precipitation, and (E) solid-state grinding for 15 min.

BAPP–β-CD prepared by the co-precipitation method due to a mixture of ICs and β-CD. Further, a cumulative XRD pattern was represented to distinguish between the physical mixture and solid ICs of β-CD with ODA and MDA (Fig. S6e). In this figure physical mixture exhibited an overlapping diffraction pattern different from solid ICs. It is worth mentioning that solid crystals of all the ICs except BAPP–β-CD were obtained from the filtrate portion, which could reduce the emergence of unwanted peaks generated from the insoluble portion (diamines). However, there is a possibility of the emergence of unthreaded β-CD peaks with ICs prepared by a high molar feed ratio.

Determination of complexation stoichiometry by Job's method

Job's plot was used to determine the host-guest ratio of ICs in the solution.[20] To do so, the total concentration of aromatic diamines and β-CD were kept constant and the molar concentration of both aromatic diamines and β-CD was changed. UV analysis was carried out for a series of complex mixtures containing mole fraction range 0.1–0.9 of each component.

COLOR Online / B&W in Print

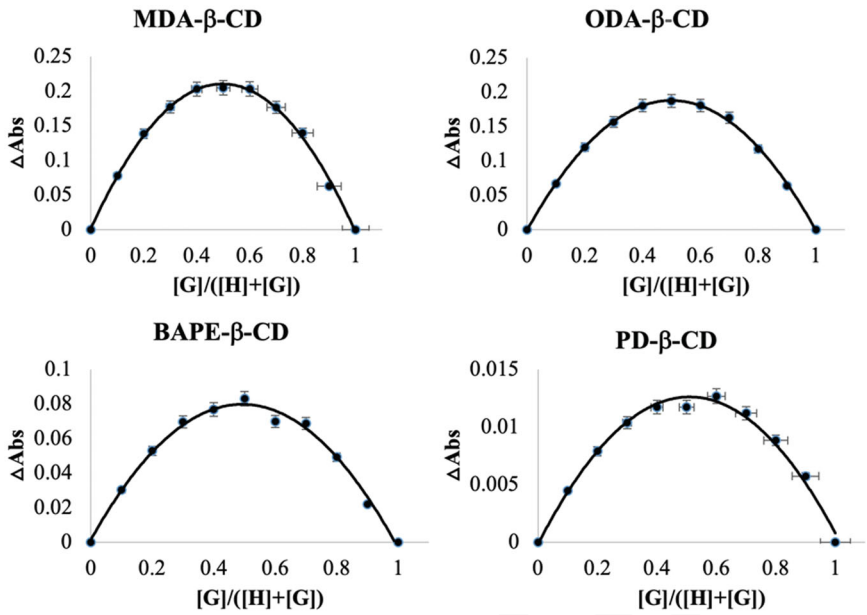

Figure 5. Job's plot of MDA-β-CD, ODA-β-CD, BAPE-β-CD, and PD-β-CD.

Stoichiometry of the ICs was determined by plotting the mole fraction of aromatic diamines *vs.* absorbance difference in a graph. The largest changes in absorbance were observed for ODA/β-CD, MDA/β-CD, BAPE/β-CD, and PD/β-CD at mole fraction 0.5, indicating the 1:1 host-guest complexes were formed (Fig. 5).[18] Further, NMR titration of PD/β-CD, MDA/β-CD, and BAPE/β-CD complexation study confirmed the formation of 1:1 ICs. On the other hand, a 1:1 complex was observed between BAPP and β-CD, which is presumably due to the 3 D bend structure of BAPP that constrain the threading of multiple β-CD (Fig. S7). Similarly, a coverage ratio of 1:1 was observed in the ^{1}H NMR spectrum of BAPP–β-CD prepared by mixing in the hot water method indicating the IC structure of BAPP–β-CD (Fig. S2r). Similarly, BAPB/β-CD stoichiometry was also found 1:1 (Fig. S7). Notably, UV analyses of BAPE, BAPB, and BAPP were carried out in 40% THF due to low solubility and precipitation problems in water. The high percentage of THF could limit the actual threading yield. Experimental conditions and UV spectrums were represented in supporting information (Table S2 and Figs. S7a–f).

Elemental analysis results of ICs

Elemental analysis was used to confirm the compositions of each molecule and coverage ratios of the IC crystals. In the elemental composition, the presence of nitrogen indicated IC formation between β-CD and aromatic diamines. Notably, a certain amount of water was embedded in the IC

Table 2. Elemental compositions of ICs and mixture.

Compound	Expected calculation (C/H/N/O)[a]	Experimental (C/H/N/O)[b]	Coverage ratio of ICs (β-CD: guest)[c]
ODA–β-CD	46.7/6.4/2.0/45.0 $C_{54}H_{82}N_2O_{36}\cdot 3H_2O$	46.6/6.4/2.0/45.0	1:1
MDA–β-CD	47.0/6.6/2.0/44.4 $C_{55}H_{84}N_2O_{35}\cdot 4H_2O$	46.4/6.45/2.0/45.1	1:1
BAPE–β-CD	41.9/6.7/0.7/50.7 $C_{140}H_{226}N_2O_{127}\cdot 20H_2O$	40.6/6.4/1.0/52.0	3:1 (mixture)
BAPB–β-CD	42.8/6.6/0.6/50.7 $C_{184}H_{296}N_2O_{142}\cdot 10H_2O$	40.1/6.5/0.7/52.8	4:1 (mixture)
PD–β-CD	45.1/6.5/2.2/46.3 $C_{48}H_{78}N_2O_{35}\cdot 2H_2O$	46.4/6.5/2.0/45.1	1:1
BAPP–β-CD	48.0/6.9/1.6/43.6 $C_{69}H_{96}N_2O_{37}\cdot 10H_2O$	48.2/5.9/1.7/44.2	1:1

[a]Calculated from formulas including water.
[b]Determined by elemental analysis.
[c]Coverage ratio was calculated based on experimental results.

crystals and mixture owing to the outer hydrophilic surface of the CDs. Considering the number of CDs threaded onto the guest molecule and hydrated water, the theoretical elemental compositions were calculated and correlated with the experimental data (Table 2). From the experimental elemental compositions, the coverage ratio or the number of guests included in the host cavity was calculated. The PD–β-CD, ODA–β-CD, and MDA–β-CD ICs showed a 1:1 coverage ratio, which is consistent with the coverage ratio calculated by ^{1}H NMR measurement and Job's plot method. The BAPP–β-CD showed a coverage ratio of 1:1, indicating one β-CD threaded onto one BAPP. Also, Job's plot determination reveals the host-guest ratio of 1:1 between β-CD and BAPP. Despite the possibilities of two β-CD threading, a 1:1 complex of BAPP–β-CD was observed. This is probably due to the 3 D bend structure of BAPP diamine as well as the polar solvent effect. In contrast, BAPE–β-CD and BAPB–β-CD showed coverage ratios of 1:3 and 1:4, respectively, which differed from the initial feed ratios (1:1, BAPE: β-CD and 1:2, BAPB: β-CD). Such high β-CD content is associated with a mixture of ICs and excess amounts of β-CD. The host: guest integral ratios in the ^{1}H NMR spectra indicated similar coverage ratios (Figs. S2g–i).

DSC analysis of ICs

DSC analysis is broadly used to study the interactions of various components of CDs ICs. ICs formation can be evidenced by the change in peak positions or evolution of new peaks. The melting behavior of the ICs was studied by DSC analysis. Typically, distinct sharp melting peaks are observed for aromatic diamines. In general, CDs crystals are in the hydrated state containing both cavity water and outer surface water. CDs dissolution in water is an endothermic process. Therefore, a broad

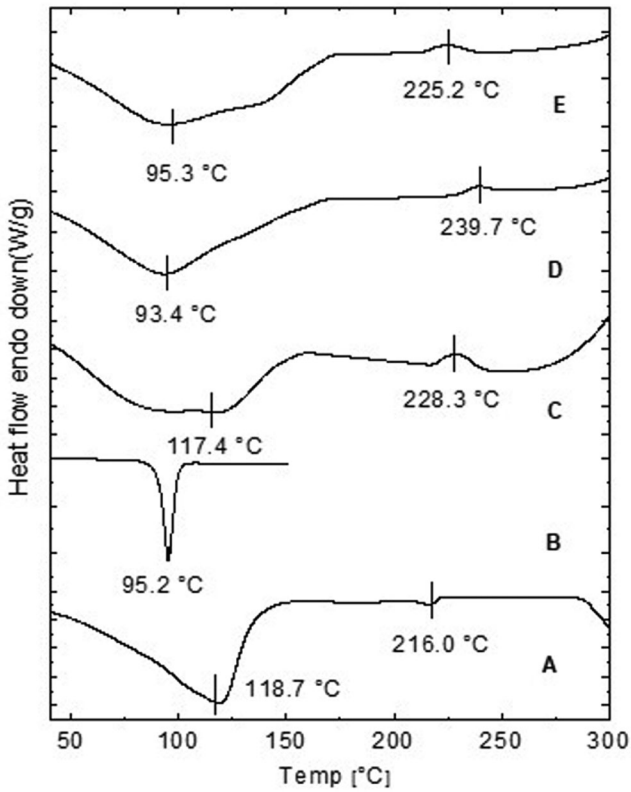

Figure 6. DSC spectra of (A) β-CD, (B) MDA, and MDA-β-CD prepared by (C) mixing in hot water, (D) co-precipitation, and (E) solid-state grinding for 15 min.

endothermic peak was observed at ~118.7 °C due to the dissolution of hydrated β-CD crystals (Fig. 6).[31,32] In the β-CD thermogram, a small endothermic peak was observed at ~216.0 °C, which could be associated with a small transformation. Typically, β-CD threading onto diamines causes suppression of diamine peaks.[18] Therefore, no sharp melting peak was observed for MDA–β-CD ICs prepared by three methods. However, a broad peak was observed for MDA–β-CD ICs due to the desorption of residual water from hydrated crystals during heat flow. Instead of the second endothermic peak of β-CD, an exothermic peak was observed for MDA–β-CD ICs, which reveals the topological transformation by the inclusion of aromatic diamines.[4,25] Similar phenomenon was observed for ODA–β-CD ICs (Fig. S8). Instead of, sharp melting peaks a broad peak at 112.6 °C difference from the β-CD peak was observed for BAPE–β-CD prepared in hot water (Fig. S8a). In contrast, a small sharp peak stemmed in BAPE–β-CD prepared by co-precipitation, which is possibly due to partially threaded BAPE. Notably, major DSC peaks of BAPE–β-CD and BAPB–β-CD prepared by solid-state grinding methods were identical with

β-CD, which reveals that the total composition was β-CD (Figs. S8a,b). Moreover, solid-state grinding produced a very small amount of threaded BAPE and BAPB. On the other hand, no typical sharp melting peak of PD and BAPP diamine was observed in DSC thermograms of PD–β-CD and BAPP–β-CD, which indicated the β-CD threaded structure of BAPP–β-CD (Fig. S8d).

TGA analysis of ICs

TGA measurement was carried out to study the weight loss and decomposition phenomenon of ICs. TGA thermograms of the studied diamines, β-CD, and ICs were represented in supporting information (Figs. S9a–e). About 99% weight loss was observed for all studied diamines up to temperature 500 °C except PD, in which total degradation occurred within 250 °C. In contrast, β-CD showed two weight-loss areas, ∼11.0% initial weight loss at 109 °C was observed due to loss of cavity water and outer surface water followed by ∼68.7% weight loss at 500 °C to furnish residual char. CD degradation involves the desorption of both cavity water and outer surface water above 100 °C followed by ring-opening (loss of glycosidic linkages), dehydroxylation (tar formation), and carbonization (char formation) at 200–500 °C.[31,32] All the ICs exhibited two major weight loss areas in the range of 200–400 °C, leading to total weight losses of 60–70%, which is less than observed for the individual diamine and β-CD, indicating that the distribution of aromatic diamines and β-CD in the total composition of ICs. Notably, about 52–58% weight loss was recorded for PD–β-CD prepared by three methods. In this case, the final degradation temperature of PD–β-CD was larger than the PD degradation temperature. In contrast, up to ∼70% weight loss was observed for BAPP–β-CD at 400 °C, which is less than the total weight loss of BAPP. Notably, the final degradation temperature of BAPP is higher than ICs prepared by three methods.

Conclusion

In this paper, a comparative study of ICs formation between β-CD and some aromatic diamines has been carried out by mixing in hot water, co-precipitation, and solid-state grinding to rationalize the most suitable method. Among three methods, ICs formation by mixing in hot water was found to be reliable as in this case co-solvent was avoided and a simple synthesis process was adopted. Solid-state grinding is also an effective method of β-CD-ICs formation of studied diamines. However, low yield and the mixture of IC and excess components are two issues for large guest

molecules. In such cases, a combination between solid-state grinding and mixing in hot water could be further investigated. The overall spectroscopic assessment confirmed the ICs formation between β-CD and aromatic diamines (PD, ODA, and MDA). However, a mixture of β-CD and IC was observed for BAPP, BAPE, or BAPB, which could be further assessed for purification. In many cases, the co-precipitation method is chosen preferentially as a synthesis process of ICs of sparingly soluble guests with CDs host before study in water or solid-state grinding methods. In those cases, ICs formation could be studied in water. It is worth noting that, the ICs we studied could be potentially studied for the preparation of the nitrogen-based thermosetting polymer. Further ICs formation of ODA could be studied to purify ODA from a crude mixture in the industrial process.

Materials and methods

Materials

ODA, BAPP, and PD were purchased from TCI and had purities of >98%. BAPE and BAPB are prepared according to the procedure mentioned in the reference.[14] MDA and β-CD were purchased from Kanto Chemical Co., Inc.

Synthesis procedure of ICs by mixing in hot water method

A 100-mL big neck oval-shaped round-bottom flask, β-CD (2.85 g, 2.51 mmol) was dissolved in 30 mL deionized water at 80 °C in an oil bath for 15 min to stabilize. ODA (0.50 g, 2.49 mmol) was added portion-wise (five portions, ∼0.10 g portion each time) as solid to the flask at 30 min intervals and stirred magnetically at high-speed. After adding the final portion reaction continued for two different times, such as 6 and 24 h, respectively at 80 °C. Flask was cooled to room temperature (24 °C). The ODA-β-CD complex solution was filtered and washed with an extra 6–8 mL of deionized water then transferred into a petri dish by a pipette and concentrated by heating at 50 °C (4–5 ml solution or maintaining the saturation level). After that, the concentrated solution was transferred into a round bottom flask and kept for crystallization in the refrigerator. To avoid the loss of complex solution in petri dish evaporation, another process was introduced to evaporate excess water by air blowing on the liquid surface by using a small diaphragm pump. In this process, a complex solution cooled to 24 °C was filtered, and washed with 6–8 mL of deionized water into a 100 ml round bottom flask and to the liquid surface air blown by a small diaphragm pump while stirring magnetically at 50 °C. Crystallization was observed after 1 h and continued for 48 h then filtered and washed by

6–8 mL deionized water then dried initially in the rotary evaporator at 50 °C then under a vacuum of 1.1 torrs, at 40 °C for 24 h. After filtering the crystal filtrate again concentrated to 6–8 mL and kept in the refrigerator to obtain further crystallization. Less than 5% of crystals were isolated for ODA-β-CD in the second crystallization. Notably, to obtain good crystals small portion of the filtered complex solution is stored in the test tube for 15-30 days. Similar, the procedure adopted for PD-β-CD, MDA-β-CD, BAPP-β-CD, BAPE-β-CD, and BAPB-β-CD. Notably, a clear solution was observed during the complexation reaction of ODA-β-CD, MDA-β-CD, BAPE-β-CD, BAPB-β-CD, PD-β-CD at 80 °C except BAPP-β-CD in which precipitation occurred during the complexation process. Apart from that some ratio complexes of ODA-β-CD (host: guest, 1:1, 1.5:1, 2:1, 2.5:1, and 3:1) and BAPE-β-CD (host: guest, 1:1, 2:1, 2.5:1, and 3:1) were prepared by similar procedure and weight percent yield is calculated based on integral ratio (IgR) factor of anomeric protons to aromatic protons and tabulated in the Table S1.

Synthesis procedure of ICs by co-precipitation method

A 50-mL big neck oval-shaped round-bottom flask, β-CD (0.29 g, 0.25 mmol) was dissolved in 7 mL deionized water and heated at 50 °C in an oil bath for 15 min to stabilize then cool to room temperature. ODA (0.05 g, 0.25 mmol) was dissolved in 3 mL methanol. ODA mixture was added into β-CD solution by a pipette dropwise while stirring magnetically. The reaction mixture was kept stirring at 24 °C for 24 h. After 24 h the mixture turned into a hazy mixture. The resultant mixture was kept for precipitation in the refrigerator for 48 h. The precipitate was filtered and rinsed with 4 mL water then dried initially in the rotary evaporator at 50 °C and then under vacuum for 24 h. The resultant solid IC was collected and used for spectroscopic assessment.

Synthesis procedure of ICs by solid-state grinding method

β-CD (0.36 g, 0.31 mmol) and ODA (0.06 g, 0.31 mmol) were taken in a mortar and added 0.25 mL of water to that mixture. The resultant slurry mixture was ground by a pastel for 15 min. Notably, every 3 min solid mixture was accumulated by spatula. After 15 min the solid mixture was collected in a 50 mL flask. The remaining solid in the mortar and pastel was rinsed with 1 mL water three times then the total mixture was suspended in 7 mL water to make a 10 mL volume. The resultant solution was heated at 50 °C in an oil bath for 30–60 min to solubilize the ICs. The suspension was filtered after cooling at room temperature then concentrated in a 4 ml

solution and kept in the refrigerator for crystallization. Crystals appeared within 5 h and continued for a further 48 h. Crystals were filtered and rinsed with 4 mL of water and dried initially in the rotary evaporator at 50 °C then under a vacuum of 1.1 torrs, at 40 °C for 24 h.

Methods

^{1}H (400.13 MHz) and ^{13}C (100 MHz) NMR spectra were recorded on a Bruker Advance Ultra Shield 400 (400.13 MHz) instrument (Bellerica, USA) using D_2O with 2,2-dimethy-2-silapentane-5-sulfonate-d_6 sodium salt (DSS-d_6) as internal standard and DMSO-d_6 solvents with tetramethylsilane as internal standard. Data for ^{1}H NMR are reported as chemical shift (δ ppm), multiplicity (s = singlet, d = doublet, t = triplet, q = quartet, m = multiplet), coupling constants (Hz), integration. Further, 2 D ROESY NMR was recorded in both D_2O and DMSO-d_6 solvents to observe the correlation peaks. Elemental analysis was carried out on an EA1112 elemental analyzer (Thermo Electron, USA). Wide-angle XRD patterns of powder samples were recorded under ambient conditions on an XRD RINT-2200 instruments (Rigaku, Japan) equipped with a Cu K ($\lambda = 1.54$ Å) source. DSC measurements were performed on a DSC-60 pulse instrument (Shimadzu, Japan) at a heating rate of 10 °C/min and an Ar flow rate of 25 mL/min using a temperature range of 40–300 °C. TGA-DTA (DTG-60A, Shimadzu, Japan) measurements were performed in a flow of Ar (25 mL/min) at a heating rate of 10 °C/min within a temperature range of 30–400 °C. Solid-state FTIR spectra were recorded on an FT/IR-6300 spectrometer (JASCO Corporation, Japan; power = 180 W, working range = 700–4000 cm^{-1}, 92 scans accumulated) at 25 °C using the ATR method. UV spectra were recorded on a UV spectrophotometer (V-630 spectrophotometer, JASCO Corporation, Japan).

Acknowledgments

All major measurements were carried out at the Hamamatsu Centre for Instrumental Analysis, Shizuoka University. We thank the director of this center and its technical staff, including Mr. Makoto Ishikawa, Mrs. Aki Miyake, Mr. Hiroki Kusanagi, and Mr. Toshihiro Hayakawa for technical support with the analyses. We are also grateful to Dr. Kohei Sato and Dr. Tetsuya Suzuki for their intellectual support at all stages of this research.

Author contributions

M.J.H., M.T., and N.M.: conceptualization. M.J.H. and M.T.: methodology. M.J.H.: software. M.J.H., M.T., and N.M.: validation. M.J.H.: formal analysis. M.J.H., M.T., and N.M.: investigation, resources, and data curation. M.J.H.: writing-original draft preparation. M.J.H., M.T., and N.M.: writing-review and editing. M.J.H.: visualization. M.T. and N.M.:

supervision. M.J.H., M.T., and N.M.: project administration. M.T. and N.M.: funding acquisition.

Disclosure statement

There are no conflicts to declare.

ORCID

Mohammed Jabedul Hoque http://orcid.org/0000-0002-4994-3654
Mitsuo Toda http://orcid.org/0000-0002-9790-2320

References

[1] Szejtli, J. Introduction and general overview of cyclodextrin chemistry. *Chem. Rev.* **1998**, *98*(5), 1743–1753. doi:10.1021/cr970022c.

[2] Crini, G. Review: a history of cyclodextrins. *Chem. Rev.* **2014**, *114*(21), 10940–10975. doi:10.1021/cr500081p.

[3] Harada, A.; Takashima, Y.; Nakahata, M. Supramolecular polymeric materials via cyclodextrin-guest interactions. *Acc. Chem. Res.* **2014**, *47*(7), 2128–2140. – doi:10.1021/ar500109h.

[4] Harada, A.; Hashidzume, A.; Yamaguchi, H.; Takashima, Y. Polymeric rotaxanes. *Chem. Rev.* **2009**, *109*(11), 5974–6023. doi:10.1021/cr9000622.

[5] Shimomura, T.; Yoshida, K. I.; Ito, K.; Hayakawa, R. Insulation effect of an inclusion complex formed by polyaniline and β-cyclodextrin in solution. *Polym. Adv. Technol.* **2000**, *11*(8–12), 837–839. doi:10.1002/1099-1581(200008/12)11:8/12<837::AID-PAT61>3.0.CO;2-B.

[6] Jarroux, N.; Guégan, P.; Cheradame, H.; Auvray, L. High conversion synthesis of pyrene end functionalized polyrotaxane based on poly(ethylene oxide) and alpha-cyclodextrins. *J. Phys. Chem. B* **2005**, *109*(50), 23816–23822. doi:10.1021/jp054908t.

[7] Yang, J. Y.; Jung, B. T.; Suh, D. H. A simple attempt to change the solubility of polyimide by physical inclusion with β-cyclodextrin and its derivatives. *Polymer* **2001**, *42*(20), 8349–8354. doi:10.1016/S0032-3861(01)00337-8.

[8] Wenz, G.; Steinbrunn, M. B.; Landfester, K. Solid state polycondensation within cyclodextrin channels leading to watersoluble polyamide rotaxanes. *Tetrahedron* **1997**, *53*(45), 15575–15592. doi:10.1016/S0040-4020(97)00980-0.

[9] Akae, Y.; Sogawa, H.; Takata, T. Effective synthesis and modification of α-cyclodextrin-based [3]rotaxanes enabling versatile molecular design. *Eur. J. Org. Chem.* **2019**, *2019*(22), 3605–3613. doi:10.1002/ejoc.201900362.

[10] Samal, S.; Choi, B. J.; Geckeler, K. E. The first water-soluble main-chain polyfullerene. *Chem. Commun.* **2000**, *60*(15), 1373–1374. doi:10.1039/b003881o.

[11] García, J. M.; Jones, G. O.; Virwani, K.; McCloskey, B. D.; Boday, D. J.; Ter Huurne, G. M.; Horn, H. W.; Coady, D. J.; Bintaleb, A. M.; Alabdulrahman, A. M. S.; et al. Recyclable, strong thermosets and organogels via paraformaldehyde condensation with diamines. *Science* **2014**, *344*(6185), 732–735. doi:10.1126/science.1251484.

[12] Lei, H.; Wang, S.; Liaw, D. J.; Cheng, Y.; Yang, X.; Tan, J.; Chen, X.; Gu, J.; Zhang, Y. Tunable and processable shape-memory materials based on solvent-free, catalyst-

free polycondensation between formaldehyde and diamine at room temperature. *ACS Macro Lett.* **2019**, *8*(5), 582–587. doi:10.1021/acsmacrolett.9b00199.

[13] Yuan, Y.; Sun, Y.; Yan, S.; Zhao, J.; Liu, S.; Zhang, M.; Zheng, X.; Jia, L. Multiply fully recyclable carbon fibre reinforced heat-resistant covalent thermosetting advanced composites. *Nat. Commun.* **2017**, *8*, 14611–14657. doi:10.1038/ncomms14657.

[14] Meador, M. A. B.; Malow, E. J.; Silva, R.; Wright, S.; Quade, D.; Vivod, S. L.; Guo, H.; Guo, J.; Cakmak, M. Mechanically strong, flexible polyimide aerogels cross-linked with aromatic triamine. *ACS Appl. Mater. Interfaces* **2012**, *4*(2), 536–544. doi:10.1021/am2014635.

[15] Inoue, Y.; Hirano, A.; Murata, I.; Kobata, K.; Kanamoto, I. Assessment of the physical properties of inclusion complexes of forchlorfenuron and γ-cyclodextrin derivatives and their promotion of plant growth. *ACS Omega* **2018**, *3*(10), 13160–13169. doi:10.1021/acsomega.8b01505.

[16] Ikeda, N.; Inoue, Y.; Ogata, Y.; Murata, I.; Meiyan, X.; Takayama, J.; Sakamoto, T.; Okazaki, M.; Kanamoto, I. Improvement of the solubility and evaluation of the physical properties of an inclusion complex formed by a new ferulic acid derivative and γ-cyclodextrin. *ACS Omega* **2020**, *5*(21), 12073–12080. doi:10.1021/acsomega.0c00277.

[17] Periasamy, R. A systematic review on the significant roles of cyclodextrins in the construction of supramolecular systems and their potential usage in various fields. *J. Carbohydr. Chem.* **2020**, *39*(5–6), 189–216. doi:10.1080/07328303.2020.1792919.

[18] Periasamy, R.; Nayaki, S. K.; Sivakumar, K.; Ramasamy, G. Synthesis and characterization of host-guest inclusion complex of β-cyclodextrin with 4,4′-methylenedianiline by diverse methodologies. *J. Mol. Liq.* **2020**, *316*, 113843. doi:10.1016/j.molliq.2020.113843.

[19] Maniam, S.; Cieslinski, M. M.; Lincoln, S. F.; Onagi, H.; Steel, P. J.; Willis, A. C.; Easton, C. J. Molecular fibers and wires in solid-state and solution self-assemblies of cyclodextrin [2]rotaxanes. *Org. Lett.* **2008**, *10*(10), 1885–1888. doi:10.1021/ol8002145.

[20] Hirose, K. A practical guide for the determination of binding constants. *J. Incl. Phenom. Macrocycl. Chem.* **2001**, *39*(3/4), 193–209. . doi:10.1023/A:1011117412693.

[21] Karthika, S.; Radhakrishnan, T. K.; Kalaichelvi, P. A review of classical and non-classical nucleation theories. *Cryst. Growth Des.* **2016**, *16*(11), 6663–6681. doi:10.1021/acs.cgd.6b00794.

[22] Rontoyianni, A.; Mavridis, I. M. Dimeric complex of alpha cyclodextrin with 1,12-diaminododecane. comparison with other alpha cyclodextrin dimeric complexes. *Supramol. Chem.* **1999**, *10*(3), 213–218. doi:10.1080/10610279908559287.

[23] Jug, M.; Mura, P. A. Grinding as solvent-free green chemistry approach for cyclodextrin inclusion complex preparation in the solid state. *Pharmaceutics* **2018**, *10*(4), 189. doi:10.3390/pharmaceutics10040189.

[24] Schneider, H. J.; Hacket, F.; Rüdiger, V.; Ikeda, H. NMR studies of cyclodextrins and cyclodextrin complexes. *Chem. Rev.* **1998**, *98*(5), 1755–1785. doi:10.1021/cr970019t.

[25] Bhattacharya, P.; Sahoo, D.; Chakravorti, S. Photophysics and structure of inclusion complex of 4,4-diaminodiphenyl sulfone with cyclodextrin nanocavities. *Ind. Eng. Chem. Res.* **2011**, *50*(13), 7815–7823. doi:10.1021/ie2004797.

[26] Harata, K. Cyclodextrins: introduction. *Chem. Rev.* **1998**, *98*, 1741–1742.

[27] Giastas, P.; Mourtzis, N.; Yannakopoulou, K.; Mavridis, I. M. Pseudorotaxanes of β-cyclodextrin with diamino end-functionalized oligo-phenyl and -benzyl compounds in solution and in the solid state. *J. Incl. Phenom.* **2002**, *44*(1/4), 247–250. doi:10.1023/A:1023029912938.

[28] Kučáková, K.; Dolenský, B. Molecular structure study of a heptakis(2,3,6-tri-O-methyl)-β-cyclodextrin complex of cholesterol. *Steroids* **2020**, *155*, 108555. doi:10.1016/j.steroids.2019.108555.

[29] Tošner, Z.; Aski, S. N.; Kowalewski, J. Rotational dynamics of adamantanecarboxylic acid in complex with β-cyclodextrin. *J. Incl. Phenom. Macrocycl. Chem.* **2006**, *55*(1–2), 59–70. doi:10.1007/s10847-005-9019-4.

[30] Nomimura, S.; Osaki, M.; Takashima, Y.; Yamaguchi, H.; Harada, A. Formation of inclusion complexes of poly(hexafluoropropyl ether)s with cyclodextrins. *Chem. Lett.* **2018**, *47*(3), 322–325. doi:10.1246/cl.171112.

[31] Trotta, F.; Zanetti, M.; Camino, G. Thermal degradation of cyclodextrins. *Polym. Degrad. Stab.* **2000**, *69*(3), 373–379. doi:10.1016/S0141-3910(00)00084-7.

[32] Specogna, E.; Li, K. W.; Djabourov, M.; Carn, F.; Bouchemal, K. Dehydration, dissolution, and melting of cyclodextrin crystals. *J. Phys. Chem. B* **2015**, *119*(4), 1433–1442. doi:10.1021/jp511631e.